Standoff Midwave Infrared Hyperspectral Imaging of Ship Plumes

Characterization of ship plumes is very challenging due to the great variety of ships, fuel, and fuel grades, as well as the extent of a gas plume. In this work, imaging of ship plumes from an operating ferry boat was carried out using standoff midwave (3-5 μm) infrared hyperspectral imaging. Quantitative chemical imaging of combustion gases was achieved by fitting a radiative transfer model. Combustion efficiency maps and mass flow rates are presented for carbon monoxide (CO) and carbon dioxide (CO_2). The results illustrate how valuable information about the combustion process of a ship engine can be successfully obtained using passive hyperspectral remote sensing imaging.

Introduction

Combustion processes from ship engines are challenging to characterize. From a lab standpoint, important installations are typically required. Characterization of an operating ship is even more difficult as the installation of lab equipment may not always be possible. In this regard, passive remote sensing technologies present distinct advantages since they are non-invasive and do not involve installing any additional equipment on the ship itself. In addition to being relatively hot, exhaust gases from ship engines typically contain infrared-active molecules such as carbon dioxide (CO_2) and carbon monoxide (CO). Therefore, infrared hyperspectral remote sensing is a technique of choice for such a system [1]. However, characterization of operating ships is difficult due to the extent of the ship plume and the dynamics associated with the ship movements caused by the waves. Consequently, imaging techniques are preferred to single-point or scanning systems.

Figure 1 Visible image of the investigated ferry boat as seen from the hyperspectral sensor location.

In this paper, characterization of an operating ferry boat (see Figure 1) was carried out using standoff midwave infrared (MWIR) hyperspectral imaging (HSI). Recording was carried out during a few minutes while passengers were transiting. Temperature maps from the ship plume as well as column density maps of exhaust gases such as CO and CO_2 could be successfully determined. Combustion efficiency maps and mass flow rates were derived from these data. The results illustrate the benefits of standoff midwave infrared hyperspectral imaging as a research tool for the characterization of combustion phenomenon such as ship plumes.

Experimental Information

Telops Hyper-Cam

The Telops Hyper-Cam is a lightweight and compact hyperspectral imaging instrument that uses Fourier Transfer Infrared (FTIR) technology. The Hyper-Cam-MW Fast features a high readout speed indium-antimonide (InSb) focal plane array (FPA) detector which contains 320×256 pixels over a basic 6.4°×5.1° field of view. The spectral resolution is user-selectable up to 0.25 cm^{-1} over the 3.0 to 5.0 μm (2000 – 3333 cm^{-1}) spectral ranges. The sensor was located at a distance of 115 m from the ship leading to an effective pixel size of 16 cm^2/pixel. The instrument's field of view was narrowed down to 128×128 pixels for the measurements leading to an effective scan rate of 3 sec/datacube. A spectral resolution of 4 cm^{-1} was used giving a total of 320 spectral bands over the whole spectral range

covered by the FPA detector. Outside temperature and relative humidity were 2 °C and 66 % respectively.

Data Processing

The broadband images associated with the hyperspectral data were obtained by summing, for each pixel, the radiance measured at each wavenumber over the whole FPA detector spectral range. Column density results were obtained by solving Equation 1, where L is the measured radiance at sensor, L_{bkg} the radiance at the back of the gas plume, τ_{plume} the gas plume transmittance, L_{plume} the self-emission radiance associated with the gas plume, and L_{atm} and τ_{atm} the self-emission radiance and transmittance associated with the atmosphere respectively. Self-emission is function of the object temperature while transmittance is function of gas concentration (expressed in ppm) and path length (expressed in meters) for a defined gas.

Equation 1

$$L = \left[L_{bkg}\tau_{plume} + L_{plume}\left(1 - \tau_{plume}\right)\right]\tau_{atm} + L_{atm}(1 - \tau_{atm})$$

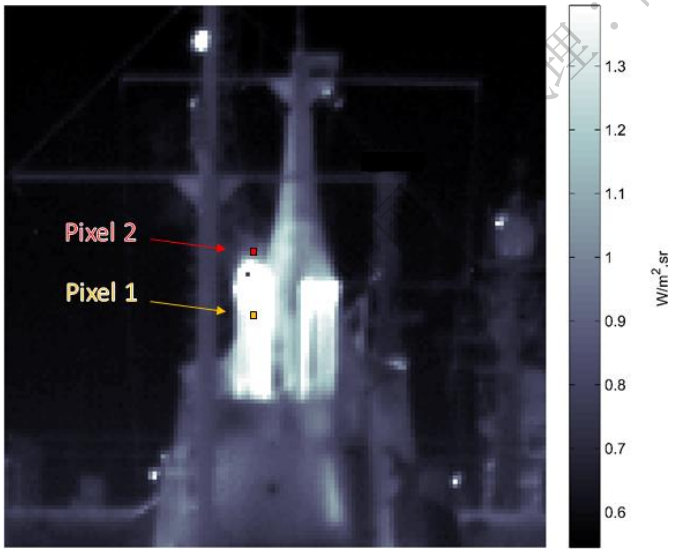

Figure 2 Broadband infrared image of a ship plume. Selected pixels are labeled for further discussion.

Results and Discussion

Midwave Infrared Remote Sensing of Combustion

A typical broadband MWIR image of a ship plume is shown in Figure 2. As expected, the chimneys are relatively warm compared with the other objects in the scene. Combustion gases can barely be seen at the exit of the chimneys even though they are present and relatively hot. Complete combustion of hydrocarbons, as in the case of diesel fuel, essentially leads to the production of water vapor (H_2O) and carbon dioxide (CO_2) as expressed in Equation 2.

Equation 2

$$C_nH_y + O_2 \rightarrow nCO_2 + {}^{y}/_{2}\,H_2O$$

It is well known that these two gases selectively absorb thus emit infrared radiation over discrete spectral ranges. Therefore, their self-emission contribution over the whole spectral response of the infrared detector is somewhat minor. The infrared spectra of two selected pixels shown in Figure 2 are presented in Figure 3A and Figure 3B in order to illustrate this aspect. The infrared spectrum associated with pixel 1 shown in Figure 3A corresponds to the chimney's body, which mostly behaves like a blackbody source. The general trend observed as a function of wavenumbers, i.e. the decaying radiance curve, corresponds to its self-emission as predicted by Planck's radiometric law. The series of sharp peaks at 2000-2100 cm^{-1}, the absorption band at 2200 cm^{-1} and the large absorption band at 2250-2400 cm^{-1} correspond to atmospheric water vapor, nitrous oxide and carbon dioxide respectively. A simulation of the atmospheric transmittance curve, carried out using weather station data and a path length of 115 m, is presented in Figure 3C for comparison purposes. Since the atmospheric gases are significantly colder than their background, i.e. the chimney's body, absorption dominates their self-emission contribution and «downward» spectral features are observed. Pixel 2 corresponds to a pixel located right above the chimney's

exit where combustion gases are expected to be present at high concentrations. Spectral features associated with hot carbon monoxide (2075-2200 cm^{-1}) and carbon dioxide (2280 and 2400 cm^{-1}) can be seen on the infrared spectrum shown in Figure 3B as well as the same atmospheric features observed in Figure 3A. The results are also consistent with previous work carried out on ship plumes [2,3]. In conditions where combustion is incomplete, combustion products such as CO, partially oxidized hydrocarbons, soot ($C_{(s)}$) or even unburnt reactants can be found as expressed in Equation 3.

Equation 3

$$C_nH_y + O_2 \rightarrow CO + H_2O + CO_2 + C_{(s)} + C_nH_xO_z$$

Since the exhaust gases are likely warmer than their background (sky radiance) and the atmosphere, self-emission dominates absorption and «upward» spectral features are observed. It is well known that the infrared spectral features of gases broaden as a function of temperature as it populates higher energy rotational levels. In the case of carbon dioxide, this effect is very significant as it can be seen in Figure 3D. From a remote sensing point of view, this broadening effect is responsible for being able to detect, identify and quantify CO_2 in the MWIR spectral range. At the atmospheric CO_2 level, only a few meters of path length are necessary to bring atmospheric transmittance down to 0 in the CO_2 spectral range as seen in Figure 3C. Since self-emission of hot CO_2 is significantly broader than what is absorbed by the somewhat colder atmospheric CO_2, only the sides of the spectral feature associated with the hot CO_2 remain. These distinct spectral features often refer to the red (2283 cm^{-1}) and blue (2288 cm^{-1}) CO_2 spikes.

Quantitative Chemical Imaging of Ship Plumes

The radiative transfer model described in Equation 1 was successfully applied to each pixel of every datacube. As seen in Figure 3B, the simulations are in good agreement with the measurements. The temperature map estimated from the model is shown in Figure 4. The temperature gradients are similar to what is expected for a ship plume as described in other works [2,3]. Column density profiles could be successfully determined for both CO and CO_2 by solving Equation 1. Only column density results (expressed in ppm×m units) can be retrieved from remote sensing since the path length is unknown and cannot be efficiently estimated from a single perspective. As seen in Figure 5 and Figure 6, the column density patterns for CO and CO_2 have the same shape than the gas plume temperature profile.

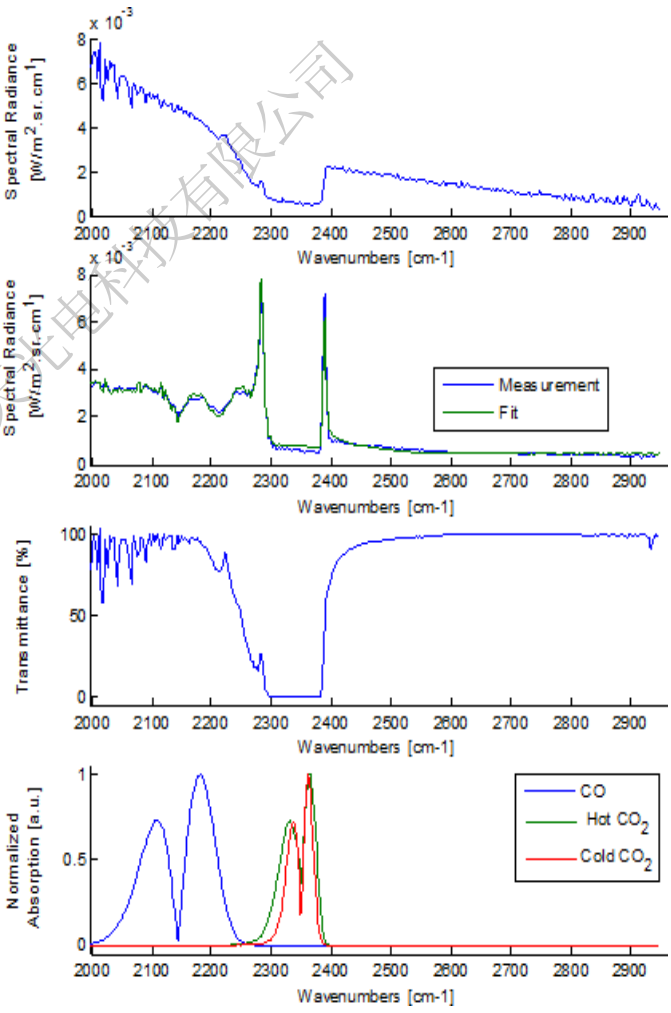

Figure 3 Infrared spectra of selected pixels are located on the chimney's body (A), away from the ship and right above the chimney's output (B). In the latter case, the measurement corresponds to the blue curve while the green curve corresponds to the best fit of Equation 1. A simulation of the atmospheric transmittance (C) and the reference spectra of carbon monoxide (CO) and carbon dioxide (CO_2) at 425 K are also presented (D) for comparison purposes.

Combustion Efficiency

It is possible to estimate the combustion efficiency maps of the ship engine using the column density quantities obtained earlier. Considering the expected combustion products from a complete (Equation 2) and incomplete (Equation 3) combustion, the total carbon mass balance can be expressed as following:

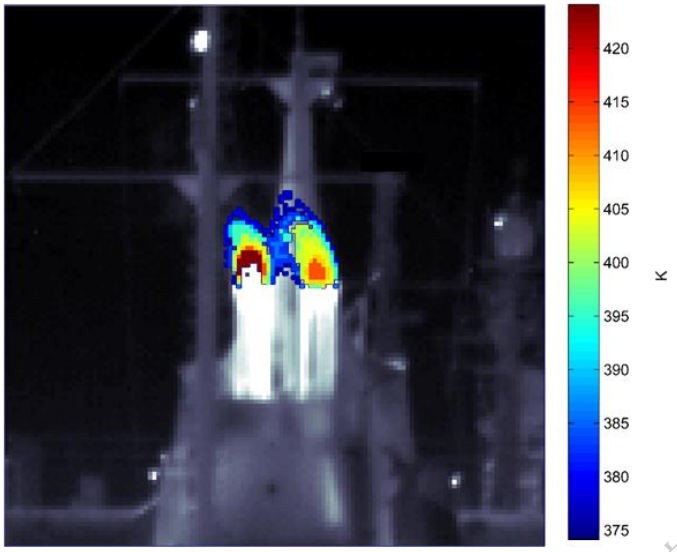

Figure 4 Gas plume temperature map associated with a single datacube of the imaging sequence derived from radiative transfer model presented in Equation 1. Temperature results are displayed over the associated broadband infrared image for clarity purposes.

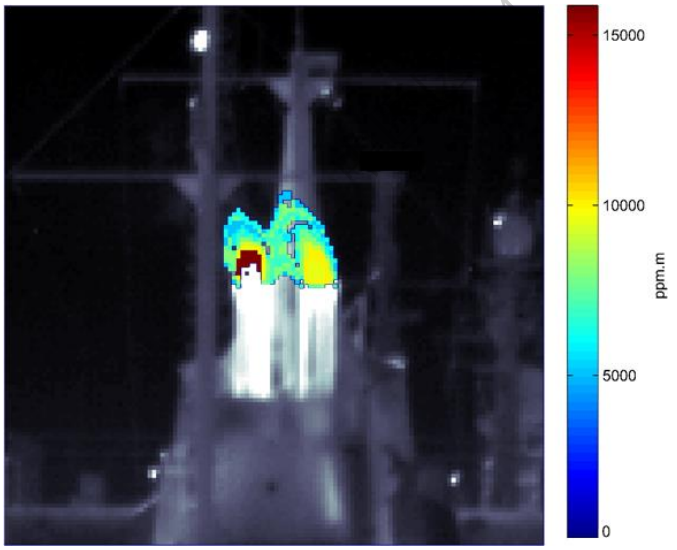

Figure 5 Carbon dioxide (CO_2) column density map associated with a single datacube of the imaging sequence. Results are displayed over the associated broadband infrared image for clarity purposes.

Equation 4

$$Comb.\ Eff. = \frac{[CO_2]}{[CO_2] + [CO] + [Hydrocarbons]}$$

By performing a ratio of the different column density quantities, there is no longer any dependency on path length. In the present case, no unburnt hydrocarbons could be detected in the exhaust gases. Their presence normally results in large spectral features in the 2850-3000 cm^{-1} spectral range which is associated with the C-H stretching vibration of hydrocarbon molecules. No such feature could be seen in any of the measurements as the one presented in Figure 3C. In addition, calculations suggest that negligible amount of soot particles, which behave like blackbodies, were present in the combustion gases. For this reason, their contribution was neglected in Equation 4. The combustion efficiency results obtained for the investigated ship plume are shown in Figure 7. As expected, the values are fairly high (> 97.5 %) suggesting that the engine combustion is very well managed in this case. Ferry boats usually run on very high grade diesel fuel, with very low sulfur content, as they maneuver near the reefs of urban areas.

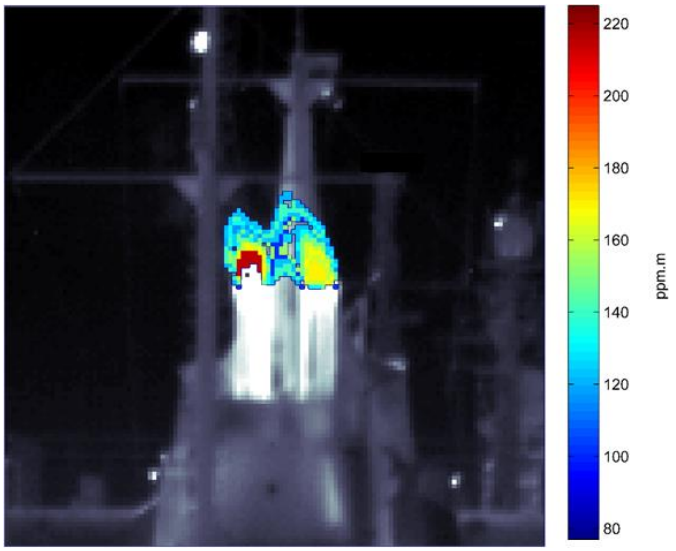

Figure 6 Carbon monoxide (CO) column density map associated with a single datacube of the imaging sequence. Results are displayed over the associated broadband infrared image for clarity purposes.

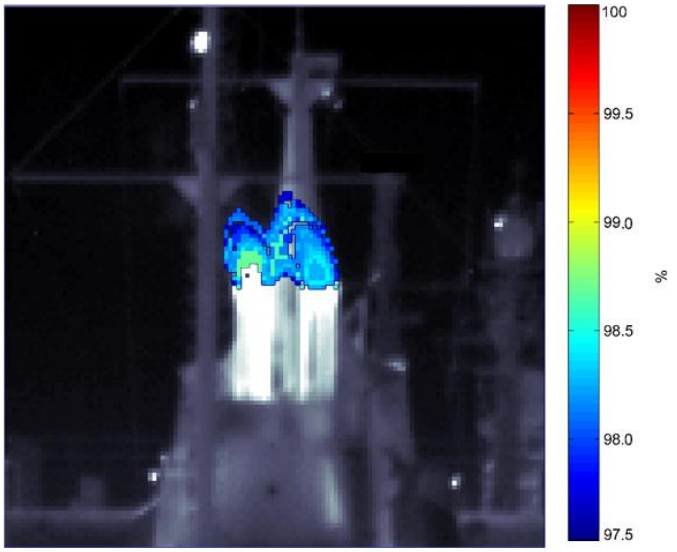

Figure 7 Combustion efficiency map associated with a single datacube of the imaging sequence. Results are displayed over the associated broadband infrared image for clarity purposes.

Mass Flow Rate

Part of the FTIR technology used in the Telops Hyper-Cam consists in collecting interferogram datacubes in a frame by frame fashion. Therefore, broadband-like infrared images are recorded at a high frame rate. Since most combustion gases are highly infrared-active molecules, significant thermal contrast associated with their displacement is observed on these images. The velocity of the combustion gases can be estimated from these high speed infrared imaging sequences using spatio-temporal correlation algorithms [4]. The mean velocity map obtained upon such procedure is presented in Figure 8. In this map, the red arrows correspond to local velocity vectors of different orientation and amplitude. As expected, the gas are exiting the ship's chimney vertically as expressed by the numerous co-aligned velocity vectors pointing upward above the chimney's output. The velocity of the combustion gases in this area was estimated to be in the range of 1 to 2 m/s.

By combining velocity (expressed in m/s) and column density (expressed in ppm×m) quantities, the dependency over path length no longer holds. Therefore, a physical quantity corresponding to linear mass flow density (expressed in kg/m.s) can be obtained for each point were the two input parameters can be successfully determined. A selection of pixels meeting these criteria is labeled in Figure 8 in order to carry out further analysis.

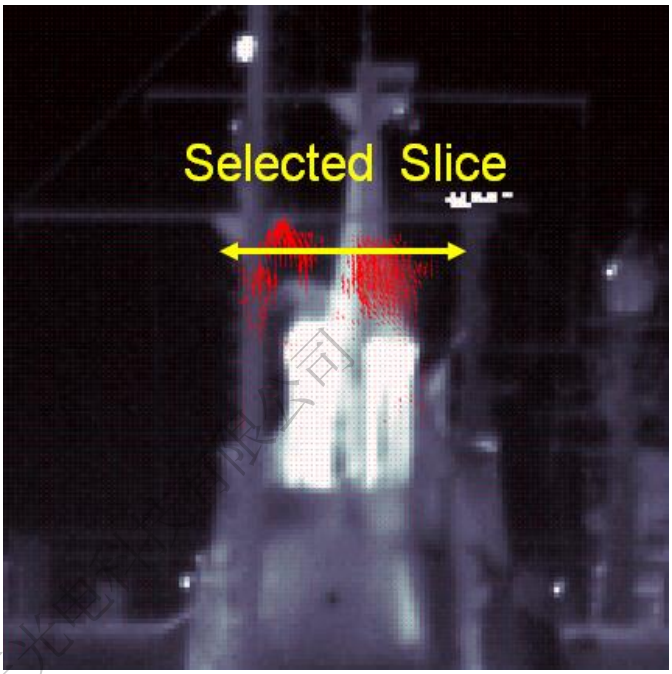

Figure 8 Velocity map obtained upon optical flow analysis. The velocity vectors (red arrows) are displayed over a representative infrared broadband image for clarity purposes. A selection of pixels where mass flow rates could be successfully determined is also shown for further discussion.

The linear mass flow density profile for CO_2, associated with the selected pixel slice above, is presented in Figure 9.

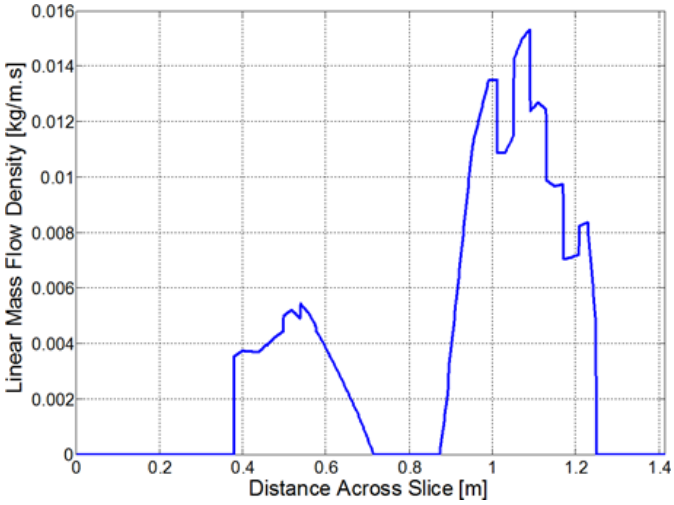

Figure 9 Linear mass flow density profile for CO_2.

As expected, the linear mass flow density increases for pixels located right above the chimney's output and maxima are obtained near the center of each chimney. By integrating these linear mass flow densities over the whole selected slice, mass flow rates are obtained for each chemical which could be successfully quantified within the gas plume. The results are presented in Table 1.

Gas	Mass flow rate [g/s]
CO	0.06
CO_2	4.8

Table 1 Mass flow rates estimated for the different combustion gases in the investigated ship plume.

The investigated ship is equipped with two MAN diesel engines. The values reported in Table 1 correspond to emissions on the order of 200 and 17 000 g/hour of CO and CO_2 respectively. These values are in good agreement with what is reported for idling ship engine of ferry boats [5].

Conclusion

Standoff MWIR infrared FTS hyperspectral imaging allows quantitative chemical imaging of ship plumes in their operating environment. It provides complete characterization in a relatively short period of time without the need of installing any additional equipment. The selectivity provided by hyperspectral technology used in the Telops Hyper-Cam allows identification and quantification of various chemicals, which can vary as a function of engines type, fuel grades, and engine revolution thereby making it a powerful investigation tool for ship plume characterization.

References

[1] P. Tremblay et al., Standoff Gas Identification and Quantification from Turbulent Stack Plumes with an Imaging Fourier-Transformed Spectrometer, Proc. of SPIE, 7673, 76730H (2010).

[2] H.M.A. et al., Ship Exhaust Gas Plume Cooling, Proc. of SPIE, 5431, 66 (2004).

[3] M. van Iersel et al., Ship Plume Modelling in EOSTAR, Proc. of SPIE, 9242, 92421S (2014).

[4] Horn, B.K.P., Schunck, B.G., Determining Optical Flow, 17, 185-203 (1981).

[5] Analysis of Commercial Marine Vessels Emissions and Fuel Consumption Data, EPA420-R-00-002 (2000).

Telops Inc.
100-2600 St-Jean Baptiste Ave
Québec (QC), Canada
G2E 6J5

Tel.: +1-418-864-7808
Fax. : +1-418-864-7843
sales@telops.com
www.telops.com